_____

UDC 544.723

ENHANCEMENT OF THE HYDROGEN SORPTION ON MESOPOROUS CARBON BY DOPING WITH PALLADIUM NANOPARTICLES

V. Gerda[1,2], G. Telbiz[3], N. Kobylinskaya[2], V. Zaitsev[2], P. Manoryk[3], J. Fraissard[1,4]

[1]*Laboratoire de Physique Quantique, Université Pierre and Marie Curie, ESPCI*
10 Rue Vauquelin, Paris 75231, France, jacques.fraissard@upmc.fr
[2]*Department of Chemistry, Shevchenko Kyiv National University*
62a Volodymyrs'ka Street, Kyiv 01033, Ukraine, nkobilinskaya@rambler.ru
[3]*Pysarzhevskiy Institute of Physical Chemistry of National Academy of Sciences of Ukraine*
31 Nauky Ave., Kyiv 03028, Ukraine, g_telbiz@yahoo.com
[4]*University Pierre and Marie Curie, 4 Place Jussieu, Paris 75005, France, jacques.fraissard@upmc.fr*

We have used the matrix synthesis protocol of Ryoo et al. for the preparation of highly ordered cubic mesoporous carbon (CMK-1) using mesoporous silica (MCM-48) as a template, in order to prepare palladium-doped CMK-1. The carbon obtained has a high surface area of 1800 m^2g^{-1}, a large porous volume of 1.14 cm^3g^{-1} and average pore diameter of 3.03 nm. Step-by-step formation of mesoporous carbon was followed by X-ray diffraction, FTIR, N2 adsorption desorption and TPD mass-spectrometry. The physical data of CMK-1 are hardly changed by Pd incorporation (CMK-1/Pd). Transmission electron microscopy and Raman spectroscopy show that the framework of the highly ordered mesoporous carbon/Pd consists of an aligned carbon phase with a graphite mode region. The potential application of CMK-1 and CMK-1/Pd as sorbents for hydrogen storage is discussed.

INTRODUCTION

In recent years, much attention has been given to the synthesis and the physicochemical properties of mesoporous [1–6] and microporous [7, 8] materials based on carbon. Carbon nanotubes as well as carbon mesoporous sieves are characterized by high values of the specific surface area and pore volume, a narrow pore diameter distribution, high thermal stability in an inert environment and high conductivity. In view of the features these ordered mesoporous carbon (CMK-1) can be used as applied materials. Using mesoporous silica as a template is particularly attractive due to the possibility of structural order and diversity in achieving novel carbon nanoarchitectures. These materials have aroused considerable interest due to their important fundamental implications and industrial applications as a potential element of different electronic nanodevices, sensors, components of selective catalysts and "containers" for the storage of hydrogen and methane [4–6].

Controlling and functionalizing carbon nanostructures are key factors in defining their applications. For example, various transition and noble metals can be supported by carbon nanostructures using the wet impregnation technique [9–14]. Indeed, carbon with a graphitic structure involves a unique metal-support interaction resulting in quite distinct catalytic behavior. For example, carbon-Pd interactions were discussed in terms of Pd particle size distribution and geometry which, in turn, are related to hydrogenation activity/selectivity [15, 16]. Experimental and theoretical investigations reveal controversies concerning the value of hydrogen storage capacity and the pore characteristics of carbon materials as well as metal loading [17–19]. In the present work ordered mesoporous carbons CMK-1 were synthesized using MCM-48 sieve as matrix according to ref [2, 5]. CMK-1 formation was followed step-by-step. The effects of finely dispersed metallic palladium on the microstructure and properties of CMK-1 were also investigated. Potential applications of CMK-1 and CMK-1/Pd as sorbents for hydrogen storage are discussed.

EXPERIMENTAL

MCM-48 silica was prepared following a hydrothermal synthesis procedure using sodium silicate as the silica source [20]. The molar composition of the starting mixture for MCM-48 synthesis was 1TEOS:0.54 NaOH:0.5 CTABr:110 H_2O. After homogenization of the mixture and hydrothermal treatment in autoclave, the product was filtered, carefully washed in water, dried at ambient tem-

perature and finally calcined in air at 823 K. After template removal, the silica was impregnated with an aqueous solution of sucrose and sulphuric acid [2, 5]. 5 mg of MCM-48 was mixed with an aqueous solution prepared from 6.25 g of sucrose, 0.7 g of H_2SO_4 and 30 ml of H_2O. The resultant mixture was dried for 5 h at 373 K and then at 443 K. After this partial carbonization, the sample was blended with a solution containing 3.75 g of sucrose, 0.4 g of H2SO4 and 30 ml of H_2O. The resultant mixture was dried again for 6 h successively at 373 and 443 K. The resultant powder was calcined and carbonized under vacuum in a quartz reactor at various temperatures (973, 1173 and 1373 K). The blackish composite was obtained in 50% ethanol. The sample was filtered, washed in ethanol and dried at 373 K. For Pd loading, 0.1 g of mesoporous carbon was mixed with $H_2[PdCl_4]$ in acetone solution, (C_{Pd2+}=1.0009 mg/ml). The volume of solution was varied depending on the degree of Pd loading required (1 and 5%). The mixture was stirred for 3 h and dried until the acetone had evaporated. XRD patterns were obtained with a CuKα source (DRON-3 M diffractometer).The hydrogen adsorption capacity was measured with a volumetric device. 100 mg of carbon sample were put in a cell immersed in a Dewar vessel with liquid nitrogen (77 K) and pure hydrogen was passed at atmospheric pressure. After 45 min the solid-hydrogen equilibrium was reached and the sample cell was isolated. The hydrogen adsorption capacity was computed from the amount of gas desorbed from the material at 313 K. This experimental procedure avoids any error related to temperature gradients between the different parts of the apparatus. The specific surface area and pore size distribution of the mesoporous materials were calculated from nitrogen isotherms at 77 K using DFT model (Micromeritics ASAP 2000) [21]. Before starting this adsorption, the samples were outgassed under vacuum at 423 K during18 hours. FTIR spectra were obtained on a BRUKER IFS 66 spectrometer. For TEM measurements, powders were deposited on a grid with a holey carbon film and transferred to a JEOL 2000 electron microscope operating at 80 kV. Changes in the amount of gas-phase products during sucrose carbonization were recorded by temperature programmed desorption monitored by a MX-7304 mass-spectrometer.

RESULTS AND DISCUSSION

Fig. 1 shows the X-ray diffraction patterns of as-synthesized and calcined MCM-48 and systematic transformation of structure during the

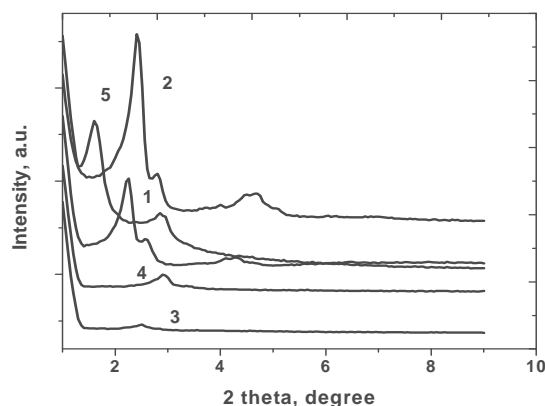removal of silica framework after carbonization of sucrose impregnated in the pores of MCM-48.

Fig. 1. XRD patterns for MCM-48 and ordered mesoporous carbon synthesized with sucrose and MCM-48 silica: *1* – MCM-48 as synthesis. *2* – MCM-48, calcined, 823 K; *3* – MCM-48, $C_{12}H_{22}O_{11}+H_2SO_4$ at 433 K; *4* – MCM-48 after vacuum carbonization at 1173K; *5* – ordered mesoporous carbon

The sharp diffraction peaks (curve *1, 2*) show a good correspondence to cubic *Ia3d* symmetry implying that the matrix is mesoporous MCM-48. The product maintained the cubic structure without collapse after calcination at 823 K demonstrating a good thermal stability. The intensity change in the XRD pattern (lattice contraction and intencity loss) illustrated that channel systems separated by the silica walls were statistically equally filled with carbon (curve *3, 4*). Structure formed in these porous systems is obviously disconnected and capable to change their position with respect to one another when the matrix is removed. When the silica walls were destructed, produced CMK-1, a new reflection corresponding of the (110) carbon networks forbidden for cubic *Ia3d* appears. This result shows change of symmetry from cubic *Ia3d* to another cubic structure *14₁32* (curve *5*), systematic transformation to new ordered mesoporous structure. The XRD of carbon material showed no patterns in the region 2θ greater than 10° indicating that the carbon framework was atomically disordered.

FTIR spectra confirmed XRD data of the systematic structural changes and show the possibility of the checking feature of the forming CMK-1 structure and illustrate all reactions and processes which pass in structure MCM-48 step by step (Fig. 2). Calcination of mesostructured matrix at 823 K (curve *2*) results in complete releasing of porous structure of MCM-48 from template, disappearance of the absorption band (V_{C-H}) characteristic for the template molecules at 2800–3000 cm^{-1}.
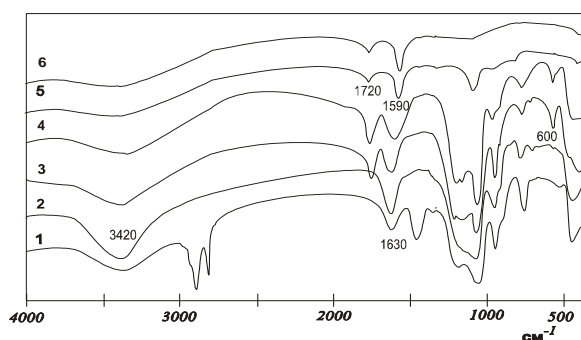
Fig 2. Infrared spectra registered after various stages of MCM-48 treatment and CMK-1 formation: *1* – as synthesized MCM-48; *2* – calcined at 823 K; *3* – after sucrose+H_2SO_4, 423 K treatment; *4* – reloaded sucrose, 433 K; *5* – carbonization in vacuum, 1173 K; *6* – final composite, after dissolved silica matrix

When the template was removed, (V_{C-H}) vibration bands disappeared and absorption bands corresponding to oscillation of physically adsorbed water at 3420 and 1630 cm^{-1} were observed.

Carbonization result in the complete destruction of structure of MCM-48 (curve *5*) and band at 1590 cm^{-1} which characterizes the unsaturated carbon structures appeared in the spectra. After dissolution of the silicate matrix (curve *6*) only absorption bands with at 1590 and 1720 cm^{-1} detected in a spectrum that can testify to the completeness of carbonization and formation of the carbon silica matrix resulted in appearance and increased of the band at 1590 cm^{-1} which characterizes the unsaturated carbon structures. After removed of silica frameworks remain only the absorption bands at 1590 and 1720 cm^{-1} that characterized formation of the mesoporous carbon remain in the spectrum.

After dissolution of the silicate matrix (curve *6*) only absorption bands with at 1590 and 1720 cm^{-1} detected in a spectrum that can testify to the completeness of carbonization and formation of carbon. The synthesis information concerning to effect of the sucrose/sulfuric acid, calcination temperature and optimum amounts of sucrose can be used for control to obtain highly ordered mesoporous carbon. With this purpose, we continuously detected r changes in the gas phase by mass spectrometer. Special attention has been paid to the formation of the volatile products which appeared at heating and carbonization sucrose in a vacuum with speed of heating 9.7 K/min in 303–1023 K.

As evidently from Fig. 3, in this temperature range the basic volatile products of thermolysis of sucrose are H_2O, CO and CO_2.
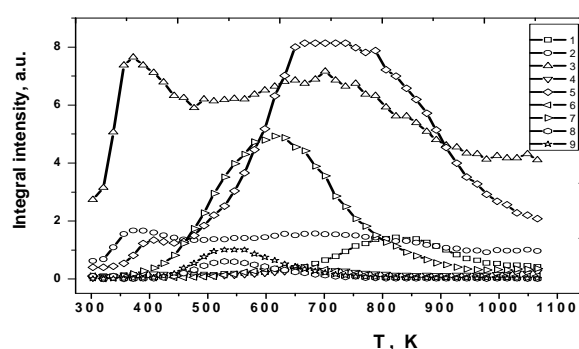

Fig. 3. Changes in the amount of gas phase products (calculated from MS data) during the reaction the sucrose carbonization for the ions with *m/z*: *1* – 15 (CH_3^+); *2* – 17 (OH^+); *3* – 18 (H_2O^+); *4* – 27 ($C_2H_3^+$); *5* – 28(CO^+); *6* – 41($C_3H_5^+$); *7* – 44 (CO_2^+); *8* – 48 (SO^+); *9* – 64 (SO_2^+)

Their liberation observed at all time heating, especially it noticeably for H_2O, CO. In case of CO_2, we observed intensive take off at 473–773 K with the maximum about 603 K. The basic process of thermodestruction of sucrose from TPDMS data begins at a temperature 450 K. Thus, at the low temperature main process of thermolysis are dehydratation and insignificant release of the CO. When the temperature increased, we detected complex process which is linked with splitting of the heterocyclic group and their destruction (CO release). Character of curves from m/z=48 and 64, corresponding SO and SO_2, at 323–613 K testify to destruction of the sulfonate group.

Interestingly, that according to TPDMS data thermolysis not completed at 1023 K, such as we detected noticeable release of H_2O and CO. Thus, we can state that for successfully completion of a process of sucrose carbonization and formation of the ordered porous carbon structure, additional treatment at a high temperature is necessary. A periodic nature of mesoporous carbon was also confirmed using Raman spectroscopy. In the visible Raman spectrum vibrational "graphite" mode appeared at 1582 and 1355 cm^{-1} bands due to highly oriented pyrolytic graphite.

Concerning the porosity, for all materials nitrogen adsorption exhibits type IV isotherms (not shown here) presenting a sharp step at a relative pressure of 0.3–0.4 attributed to capillary condensation in the ordered mesoporous structure. The results of calculations are given in Table. Pore size analysis shows that both MCM-48 and CMK-1 are structurally microporous and mesoporous but the microporosity is much less important for CMK-1. The average pore size and the

total surface area increase from 2.12 nm to 3.03 nm and from 1310 m^2/g to 1801 m^2/g for MCM-48 and for CMK-1, respectively. For the CMK-1/Pd samples, reduction of Pd with hydrogen does not change the textural/structural parameters significantly as compared with those of CMK-1 (Table). The low angle XRD patterns of CMK-1 with or without Pd are identical. The specific surface areas and volumes corresponding to the different type of pores are roughly the same. The average pore diameter has the same value (3.11 nm) but this latter corresponds in fact to a broader distribution of pore size which could result from a modification due to the influence of the solution used for Pd loading.

Analysis of TEM images reveals that the size distribution of palladium particles is quite narrow (average size 2~7 nm) and that these latter are partly dispersed within the matrix. Unfortunately, TEM shows also some large particles; especially for CMK-1/Pd 5%.These can be detected also with high-angle XRD, with a reflection characteristic of metallic palladium at 39.7 degrees. Of course, these large particles are located outside the mesopores of carbon network.

Hydrogen adsorption measurement. First we compared the results of the effective hydrogen storage by CMK-1 prepared at different temperatures and sucrose carbonization times. Hydrogen adsorption on these ordered carbon materials increases noticeably with the carbonization temperature up to 1173 K (Fig. 4).

At higher temperature, further increase up to 1373 K has the reverse effect leading to a decrease in hydrogen adsorption. These results show that the conditions of CMK-1 synthesis have a great influence on the quantity of hydrogen adsorbed by this material. The experimental data for the hydrogen capacities of MCM-48 and CMK-1 at 77 K and atmospheric pressure are presented in Table. The lowest value is obtained with MCM-48 (0.51 wt. %) while the maximum hydrogen sorption on CMK-1 is 1.80±0.04 wt. % at a carbonization temperature of 1173 K for 3 hours**.** Similar data were observed Gadiou et al. [17] in the case of ordered nanostructure carbons samples. The amounts of adsorbed hydrogen, related to the same amount of corresponding CMK-1, are 2.07 and 2.17 wt % for samples CMK-1 – 1% and 5%, respectively. The corresponding increases of hydrogen adsorption due to this doping are approximately 15% and 20% (Table).
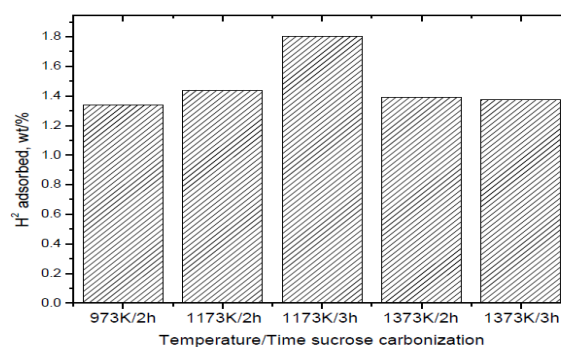

Fig. 4. Correlation between temperature/time carbonization of sucrose and storage capacity different CMK-1 at 77 K and ambient pressure

Table. Surface areas, volumes and H$_2$ capacity of the samples

Sample	MCM-48	CMK-1	Pd CMK-1 (wt. 1%)	Pd CMK-1 (wt. 5%)
S_{tot}, m^2/g	1308	1800	1794	1720
S_{micro}, m^2/g	401	156	151	133
S_{meso}, m^2/g	901	1577	1576	1522
S_{macro}, m^2/g	6	67	67	65
V_{tot}, cm^3/g	1.16	1.15	1.12	1.09
V_{micro}, sm^3/g	0.10	0.10	0.10	0.09
V_{meso}, sm^3/g	0.92	1.00	0.97	0.96
V_{macro}, sm^3/g	0.14	0.05	0.05	0.04
D, nm ±0.05	2.12	3.03	3.11	3.11
H$_2$ capacity, wt, %	0.51±0.02	1.80±0.04	2.07±0.05*	2.17±0.06*

*related to the same amount of CMK-1.

Of course, during hydrogen adsorption there is the formation of β-Pd hydride of approximate formula is Pd-H$_{0.65}$. However, expressed in wt %, this corresponding amount is negligible. This phenomenon can be attributed to the spillover effect, as was proposed in [22]. It was shown in [23] that there is always equilibrium between H$_2$ gas, H$_2$ adsorbed on the Pd surface and H$_2$ of β-Pd hydride, this latter form being at its maximum value when the surface of the particle is saturated

$$H_e \Leftrightarrow (H) \text{ adsorbed} \Leftrightarrow (H_2) \text{ gas.}$$

Consequently, there is always exchange and desorption of H species to re-form (H$_2$) gas or to diffuse throughout the carbon structure as was shown for the case of Pt supported on silica and zeolites [24, 25].

CONCLUSION

Matrix synthesis and transform during the formation of three-dimensional structure of ordered mesoporous carbon were described. The formation CMK-1 was checked by X-ray diffraction, FTIR, and TPD mass spectrometry. It was shown that for successfully completion of a process of sucrose carbonization the additional ageing at high temperature treatment is the necessary criterion. Functionalization of the ordered carbon by Pd nanoparticles resulted in increasing of adsorption of hydrogen but more surprisingly that sorptive capacity of H_2 does not depend on Pd concentration (1–5%). In addition the characterization of this volume of narrow micropores can be a good parameter for the evaluation of the hydrogen adsorption capacity of these new Pd doped and native carbon material.

REFERENCES

1. *Ryoo R., Joo S.H., Kruk M., Jaroniec M.* Ordered mesoporous carbons // Adv. Mater. – 2001. – V. 13, N 9. – P. 677–681.

2. *Kruk M., Jaroniec M., Ryoo R., Joo S.H.* Block-copolymer-templated ordered mesoporous silica: array of uniform mesopores or mesopore-micropore network? // J. Phys. Chem. B. – 2000. – V. 104, N 48. – P. 7960–7968.

3. *Sakintuna B., Yurtim Y.* Templated porous carbons: a review article // Ind. Eng. Chem. Res. – 2005. – V. 44, N 9. – P. 2893–2902.

4. *Joo S.H., Jun S., Ryoo R.* Synthesis of ordered mesoporous carbon molecular sieves CMK-1 // Microporous Mesoporous Mat. – 2001. – V. 44–45. – P. 153–158.

5. *Ryoo R., Joo S.H., Jun S.* Synthesis of highly ordered carbon molecular sieves via template-mediated structural transformation // J. Phys. Chem. B. – 1999. – V. 103, N 37. – P. 7743–7746.

6. *Schuth F.* Non-siliceous mesostructured and mesoporous materials // Chem. Mater. – 2001. – V. 13, N 10. – P. 3184–3195.

7. *Garsuch A., Klepel O.* Synthesis of ordered carbon replicas by using Y-zeolite as template in a batch reactor // Carbon. – 2005. – V. 43, N 11. – P. 2330–2337.

8. *Garnsuch A., Böhlmann W., Sattler R.R. et al.* [129]Xe NMR studies on carbon replicas of Y zeolite // Carbon. – 2006. – V. 44, N 7. – P. 1173–1179.

9. *Tiemann M.* Repeated templating // Chem. Mater. – 2008. –V. 20, N 3. – P. 961–971.

10. *Lee D., Kim H., Kang M. et al.* Efficient hydrogenation catalysts of Ni or Pd on nanoporous carbon workable in an acidic condition // Bull. Korean Chem. Soc. – 2007. – V. 28, N 11. – P. 2034–2040.

11. *Saha D., Deng Sh.* Hydrogen adsorption in ordered mesoporous carbon doped with Pt, Pd, Ru and Ni // Langmuir. – 2009. – V. 25, N 21. – P. 12550–12560.

12. *Zielinski M., Wojcieszak R., Monoeverdi S. et al.* Hydrogen storage in nickel catalysts supported on activated carbon // Int. J. Hydrogen Energy. – 2007. – V. 32, N 8. – P. 1024–1032.

13. *Huwe H., Froba M.* Synthesis and characterization of transition metal and metal oxide nanoparticles inside mesoporous carbon CMK-3 // Carbon. – 2007. – V. 45, N 2. – P. 304–314.

14. *Park S.Y., Choi B.H., Kang M. et al.* Diarylmethanes catalyzed by nickel (II) ion on nanoporous carbon // J. Mol. Catal. A. – 2007. – V. 265, N 1–2. – P. 323–329.

15. *Ros T.G., Keller D.E., van Dillen A.J. et al.* Preparation and activity of small rhodium metal particles on fishbone carbon nanofibres // J. Catal. – 2002. – V. 211, N 1. – P. 85–102.

16. *Amorin C., Keane M.A.* Palladium supported on structured and nonstructured carbon: A consideration of Pd particle size and the nature of reactive hydrogen // J. Colloid Interface Sci. – 2008. – V. 322, N 1. – P. 196–208.

17. *Gadiou R., Saadallah S., Piquero T. et al.* The influence of textural properties on the adsorption of hydrogen on ordered nanostructured carbons // Microporous Mesoporous Mater. – 2005. – V. 79, N 1–3. – P. 121–128.

18. *Orimo S., Meyer G., Fukunaga T. et al.* Hydrogen in the mechanically prepared nanostructured graphite // Appl. Phys. Lett. – 1999. – V. 75. –P. 3093–3095.

19. *Panella B., Hirscher M., Roth S.* Hydrogen adsorption in different carbon nanostructures_// Carbon. – 2005. – V. 43, N 10. – P. 2209–2214.

20. *Kresge C.T., Leonowicz M.E., Roth W.J., Beck J.S.* Ordered mesoporous molecular sieves synthesized by a liquid-crystal template mechanism // Nature. – 1992. – V. 359. – P. 710–714.

21. *Telbiz G.M., Gerda V.I., Gun'ko V.M.* Matrix synthesis and properties of the 3D-nanoordered mesoporous carbon material // Nanosystems,

Nanomaterials, Nanotechnologies. – 2005. – N 3. – P. 661–666 (in Russian).

22. *Zacharia R., Rather S., Hwang S.W., Nahm K.S.* Spillover of physisorbed hydrogen from sputter-deposited arrays of platinum nanoparticles to multi-walled carbon nanotubes // Chem. Phys. Lett. – 2007. – V. 434, N 4–6. – P. 286–291.

23. *Polisset M., Fraissard J.* ^{1}H NMR study of hydrogen adsorption on PdNaY: Influence of metal particle size // Colloids Surf. A. – 1993. – V. 72. – P. 197–206.

24. *Lenz D., Conner W.C., Fraissard J.* Hydrogen spillover on silica: III. Detection of spillover by proton NMR // J. Catal. – 1989. – V. 117. – P. 281–289.

25. *Fraissard J.* NMR studies of supported metal catalysts // Catal. Today. – 1999. – V. 51, N 3–4. – P. 481–499.

Підвищення сорбції водню допуванням мезопористого вуглецю наночастинками паладію

В.І. Герда, Г.М. Тельбиз, Н.Г. Кобилінська, В.М. Зайцев, П. Манорик, Ж. Фрайсард

*Лабораторія квантової фізики, Університет П'єра та Марії Кюрі,
вул. Вакулин10, Париж 75231, Франція, jacques.fraissard@иртс.fr
Хімічний факультет, Київський національний університет ім. Т. Шевченка
вул. Володимирська 62а, Київ 01033, Україна, nkobilinskaya@rambler.ru
Інститут фізичної хімії ім. Л.В. Писаржевського Національної академії наук України
пр. Науки 31, Київ 03028, Україна, g_telbiz@yahoo.com
Університет П'єра та Марії Кюрі, пл. Жюссьє 4, Париж 75005, Франція, jacques.fraissard@иртс.fr*

Мезопористий вуглець, допований паладієм, був одержаний шляхом матричного синтезу з використанням мезопористого кремнезему як темплату. Отримані зразки високовпорядкованого кубічного мезопористого вуглецю характеризуються питомою площею поверхні до 1800 м^2/г, великим об'ємом пор до 1,14 см^3/г і середнім діаметром від 3,03 нм. Стадії одержання мезопористого вуглецю та композитного матеріалу контролювали методами рентгенівської дифракції, ІЧ-спектроскопії з Фур'є-перетворенням, низькотемпературної адсорбції азоту та ТПД мас-спектрометрії. Встановлено, що допування зразків паладієм не приводить до руйнування структури матриці; згідно з даними просвічуючої електронної мікроскопії та спектроскопії комбінаційного розсіювання структура високовпорядкованого мезопористого композиту складається з впорядкованої вуглецевої фази з ділянками графіту і наночастинок паладію, інкорпорованого в мезопорах матриці, а композитні зразки показують підвищену сорбційну ємність по водню.

Повышение сорбции водорода допированием мезопористого угля наночастицами палладия

В.И. Герда, Г.М. Тельбиз, Н.Г. Кобылинская, В.Н. Зайцев, П. Манорик, Ж. Фрайсард

*Лаборатория квантовой физики, Университет Пьера и Марии Кюри,
ул. Вакулин,10, Париж 75231, Франция jacques.fraissard@иртс.fr
Химический факультет, Киевский национальный университет им. Т. Шевченка
ул. Владимирская 62а, Киев 01033, Украина, nkobilinskaya@rambler.ru
Институт физической химии им. Л.В. Писаржевского Национальной академии наук Украины
пр. Науки 31, Киев 03028, Украина, g_telbiz@yahoo.com
Университет Пьера и Марии Кюри, пл. Жюссье 4, Париж 75005, Франция, jacques.fraissard@иртс.fr*

Мезопористый углерод, допированный палладием, был получен методом матричного синтеза с применением в качестве темплата мезопористого кремнезема. Получены образцы высокоупорядоченного кубического мезопористого угля, которые характеризуются большой удельной площадью поверхности 1800 м^2/г, большим объемом пор до 1,14 см^3/г и средним диаметром от 3,03 нм. Стадии получения мезопористого угля и композитного материала контролировали методами рентгеновской дифракции, ИК-спектроскопии с Фурье-преобразованием, низкотемпературной адсорбции азота и ТПД масс-спектрометрии. Установлено, что допирование образцов палладием не приводит к разрушению структуры матрицы; согласно данным просвечивающей электронной микроскопии и спектроскопии комбинационного рассеивания структура высокоупорядоченного мезопористого композита состоит из упорядоченной углеродной фазы с участками графита и наночастиц палладия, инкорпорированного в мезопорах матрицы, а полученные композитные образцы показывают повышенную сорбционную емкость по водороду.